



# A Novel Condition Indicator for Bearing Fault Detection Within Helicopter Transmission

Faris Elasha<sup>1</sup> · Xiaochuan Li<sup>2</sup> · David Mba<sup>2,3</sup> · Adebayo Ogundare<sup>4</sup> · Sunday Ojolo<sup>4</sup>

Received: 5 February 2020 / Revised: 9 June 2020 / Accepted: 13 June 2020 / Published online: 22 June 2020  
© Krishtel eMaging Solutions Private Limited 2020

## Abstract

**Background** Helicopter usage and monitoring system (HUMS) is one of the critical systems for helicopter's safety and reliability. Whilst HUMS has proven to be effective in detecting gears' defects, bearing failures are not adequately detected using current monitoring indicators. Detection of bearing faults in helicopter gearboxes is made challenging by the presence of the complicated signal transmission path attenuating the monitored signal to the receiving sensor.

**Purpose** To ensure safe operation of helicopters, this research proposes a novel condition indicator to detect bearing faults in helicopter gearboxes.

**Methods** For this purpose, vibration measurements captured from a CS-29 category 'A' helicopters test rig were utilized for detecting a bearing defect that has occurred in the epicyclic module of the main gearbox. Signals of rolling element bearings under various fault conditions were collected, and an adaptive filter algorithm was utilized to separate the random component of the signal. The resultant signatures were then further processed using wavelet analysis to extract the bearing signal of interest.

**Results** Results showed that this new indicator successfully detect bearing faults. Besides, the impulse energy indicator responds consistently to the fault severity compared to the traditional indicators such as RMS and kurtosis.

**Conclusion** A technique to extract frequency band corresponding to the bearing fault impulses has been developed and tested. The technique employs the adaptive filter signal separation, wavelet packet decomposition and the combination of RMS and kurtosis to select the optimum filter band.

**Keywords** Bearing · Signal separation · Vibration · Helicopter · Gearbox · Fault detection

## Introduction

Helicopter HUMS is a sophisticated system developed to inform condition-based maintenance strategy applied to helicopters. It aims to ensure helicopter safe operation and reduce unnecessary repair cost. A typical helicopter HUMS system monitors the health of the rotor system, engines,

airframe, and transmission [1, 2]. Whilst HUMS has proven to be effective in detecting gear defects, bearing failures were not adequately detected using current monitoring indicators.

This was illustrated in an accident (2009) involving a Super-Puma helicopter in which the deterioration of a planet gear bearing had caused a loss of life. Interestingly, the HUMS monitoring system did not show any indication of an incipient fault. Although there were some trends in the vibration condition indicators (CIs) the HUMS system did not generate any alerts.

Detection of bearing faults in helicopter gearboxes is made challenging by the presence of the complicated signal transmission path attenuating the monitored signal to the receiving sensor. A separation analysis is conducted to decompose the bearing signal into deterministic and random components. The former corresponds to the gear component, and the latter corresponds to the bearing component of the obtained signal. The slip experienced by the rolling elements

✉ Faris Elasha  
faris.elasha@coventry.ac.uk

<sup>1</sup> Faculty of Engineering, Environment and Computing,  
Coventry University, Coventry, UK

<sup>2</sup> Faculty of Technology, De Montfort University, Leicester,  
UK

<sup>3</sup> Department of Mechanical and Automotive Engineering,  
Qingdao University of Technology, Qingdao, China

<sup>4</sup> Department of Mechanical Engineering, University of Lagos,  
Nsukka, Nigeria

is the main reason why the bearing's contribution to the measured signal is random [3–6]. Several studies for signal separation have been reported in the literature, each having relative merits and drawbacks [3, 7–9].

Linear prediction (LP) is one of the most popular methods for the separation of the deterministic component of a signal from the noisy random component. The drawback of LP is that its effectiveness depends on the number of past measurements used. The higher numbers of past observation over-constrain the estimation and tend to reduce even the main components of the signature, whilst smaller numbers of past observation produce a poor estimation, providing little improvement in the signal-to-noise ratio [7, 8]. It is worth noting that LP has been applied only to stationary vibration signals.

Rolling element bearing faults can cause shocks, resulting in higher resonance frequencies' excitation leading to amplitude-modulated depending on the loading distribution and transmission path [9]. As such, the analysis of a vibration signal with amplitude modulation typically involves the extraction of the frequency of these impulses. Methods such as Spectral kurtosis should be able to separate these impulses.

The spectral kurtosis (SK) was introduced in 1983 by Dwyer [10] as a spectral analysis tool to identify non-Gaussian components of a signal in the frequency domain. This method can detect the presence of “randomly occurring signals” and identify their locations in the frequency domain. It has proven to be effective in detecting bearing defects even in the presence of strong additive noise [8, 11]. Although the SK has been modified using many signal processing techniques such as wavelet, autoregressive and kurtogram, it cannot offer diagnostic advantages when employed in systems with complex transmission paths and high-speed machines. This is because the kurtosis is high only if a single impulse is separated from the vibration signal; this will be the only case for a relatively very high amplitude response at resonance with short decay time.

Recently, cyclostationary-based tools, such as the Cyclic Spectral Correlation CSC and Cyclic Spectral Coherence CSCoh, have been used as methods for bearing diagnostics of helicopter gearboxes [12, 13]. These techniques have been validated through experiments on a degradation dataset containing roller damage on a bearing mounted on a UH-60 Blackhawk helicopter Main Gearbox (MGB). The results of these methods were presented on a 2D-bi variable map. One of the axes of this map is the spectral frequency axis, and it provides information about the excitation frequencies, and the other axis is the cyclic frequency axis, presenting the characteristic modulation frequency components. Integration of these two 2D matrix results in a spectrum of the demodulated signal used for fault detection. In non-stationary operation, roller element bearing produces a series of

cyclic impacts signal locked to the shaft angle, analysis of such signals using frequency or time-domain methods is not sufficient and methods such as averaged instantaneous power spectrum and angular-temporal spectrum can be used instead [14]. These algorithms require rigorous statistical definitions enabling the use of estimators. Recently, a novel spectrum sensing technique based on the angle–time analysis has been developed to detect the nonstationary of a signal [15]. The introduced technique consists of a novel feature extractor to provide a generalised representation of the conventional cyclostationarity concept. However, interpretation of these results needs highly skilled expertise.

Therefore, this paper proposes a simple algorithm to detect bearing faults by separating the non-deterministic signal using an adaptive filter. The novel new condition indicator uses the combination indicator to detect the bearing fault and was compared to well-established indicators such as RMS and kurtosis.

The main contribution of this paper is the development of a new health indicator especially to detect the bearing defect in helicopter gearboxes. For this purpose, vibration measurements captured from a CS-29 category ‘A’ helicopters test rig were utilised for detecting a bearing defect that has occurred in the epicyclic module of the main gearbox. Signals of rolling element bearings under various fault conditions are collected, and an adaptive filter algorithm is utilised to separate the random component of the signal. The resultant signatures were then further processed using wavelet analysis to extract the bearing signal of interest.

## Bearing Condition Indicators

Helicopters health and usage monitoring systems (HUMS) are commonly used for the diagnosis of the transmission system; however, most HUMS condition indicators (CIs) used are related to gears' faults and there is a lack of CIs to identify bearing failure [16].

Due to the limited ability of HUMS' indicators to identify a range of bearing defect conditions in helicopter gearboxes, a novel condition indicator is proposed. This condition indicator is based on measuring the total energy of the impulse bursts, using a frequency band matched to the bearing signal. This indicator, called the impulse energy (IE) indicator, can be estimated by separating the bearing signal using an adaptive filter algorithm described in “\*\*\*Signal Separation and decomposition”. The non-deterministic component is further analysed using wavelet analysis to decompose the signal into certain frequency bands based on “Bark frequency scale” (also called “critical band rate” [17]), and then the combination indicator is estimated for the decomposed signals; the combination indicator aims to select one of the decomposed signals to estimate the impulse energy indicator. The latter

was estimated using Eq. (1) which is based on Parseval's theorem for energy estimation. The procedure for estimating this metric is shown in Fig. 1.

$$IE = \sum_{t=0}^{t=n} [x_t]^2 dt, \quad (1)$$

where  $x_t$  is time-domain signal with  $n$  number of samples.

The idea behind this indicator is that the bearing signal extracted by the signal processing procedure described in Fig. 1 will have high energy due to the impulses imposed by bearing failures. However, in the case of no damage, the extracted signal energy should have low energy compared to the faulty signal.

### Signal Separation and Decomposition

The signal separation was performed with an adaptive filter using the fast block least mean square algorithm (FBLMS) described by Elasha et al. [8]. The FBLMS algorithm is a computationally efficient signal separation method [18] and as such is suitable for online bearing fault diagnosis which requires an immediate response. This algorithm transforms the time signal into the frequency domain where the filter coefficients are updated; details of the procedure have been summarised in Ferrara [19].

For the purpose of this paper, the wavelet packet decomposition (WPD) was selected for signal decomposition due to its ability to detect the transient events within the signal and in dealing with signals captured from gearboxes with non-stationary characteristics. Moreover, the WPD provides signal analysis on the desired frequency sub-band, which may be used to reduce the computational burden. The wavelet packet decompositions were obtained using a series of digital filters containing high- and low-pass filter to analyse both high and low frequency. Passing the signal in first-stage filters known as the first level of decomposition, in which the signal is decomposed into high- and low-frequency parts, then each part is passed through next level of filters which decompose the signal further. This procedure is usually

repeated many times until the required number of levels has been achieved.

### Selection of Impulse Band

In this paper, the Combination indicator is presented as the criterion to select the decomposed signal related to bearing fault. In other words, the combination indicator has been used to select the frequency band for the bearing signals from the Wavelet decomposed signals. The indicator combines both Kurtosis and rms of decomposed signal. The formula is presented below:

$$CI = K = \frac{\int_{-\infty}^{\infty} [x - \mu]^4 p(x) dx}{\sigma^4} \times \sqrt{\frac{1}{N} \sum_{i=1}^N (x_i^2)}, \quad (2)$$

where  $x$  denotes the decomposed signal with average  $\mu$  and standard deviation  $\sigma$ .  $N$  represents the total number of samples in the waveforms,  $x_i$  denotes waveform samples, and  $p(x)$  is the probability density function.

This concept is proposed to enhance the accuracy of Kurtosis, when the Kurtosis fails to indicate disturbances, which particularly happens in the signal that contains very high background noise or when a non-stationary signal is involved. The condition indicator was estimated for the decomposed signals, and the signal with maximum combination indicator is then selected for impulse energy indicator estimation.

### Root Mean Square (RMS)

One commonly used statistical feature that describes key condition indicators for the gearbox is the root mean square (RMS). RMS values of vibration signals tend to provide a measurement of the overall vibration level of the damaged component. This is because vibration energy typically increases as the gearbox degrades hence higher RMS [20]. The RMS is given by

$$RMS = \sqrt{\frac{1}{N} \sum_{i=1}^N (x_i^2)} \quad (3)$$

where  $x_i$  represents waveform samples and  $N$  denotes the total number of samples in the waveforms. RMS monitoring is suitable for diagnosing slow evolving faults. However, it has been pointed out that RMS values do not increase with the isolated peaks in the signal, and as a result, this parameter is not very sensitive to incipient tooth failure. However, RMS is still one of the most frequently used health condition indicators.

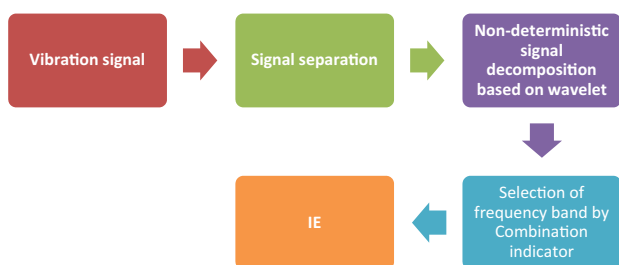


Fig. 1 Impulse energy indicator (IE) calculation procedure

## Kurtosis

Kurtosis can be defined as the normalised fourth population moment about a probability density function [21, 22]:

$$K = \frac{\int_{-\infty}^{\infty} [x - \mu]^4 p(x) dx}{\sigma^4}, \quad (4)$$

where  $\mu$  denotes the mean and  $\sigma$  is the standard deviation of the signal samples. Kurtosis widely employed in the field of gearbox diagnosis principally due to its ability to detect impulsive type signatures which can occur with bearing defects [9, 10, 23].

## Experimental Setup

The data used in this study were captured from a CS-29 Category ‘A’ helicopter gearbox test rig. Seeded defects in one of the planetary gears’ bearings of the second epicyclic stage were created. The test facility was of back-to-back rig configured and powered by two motors simulating dual-power input.

## CS-29 ‘Category A’ Helicopter Main Gearbox

A CS-29 ‘Category A’ helicopter gearbox was adopted for the experimental tests. It is visible from Fig. 2 that the transmission system of the gearbox is connected to two shafts, one from each of the two free turbine engines. The input speed specification of the MGB is around 23,000 rpm which is then reduced to the nominal main rotor speed of 265 rpm.

The main rotor gearbox consists of two sections, the main module, which reduces the input shaft speed from 23,000 rpm to around 2,400 rpm. This section includes two parallel gear stages. This combined drive provides power to the tail rotor drive shaft and the bevel gear. The bevel gear reduces the rotational speed of the input drive to 2,405 rpm and changes the direction of the transmission to drive the epicyclic reduction gearbox module. The second section is the epicyclic reduction gearbox module which is located on top of the main module. This reduces the rotational speed to 265 rpm which drives the main rotor. This module consists of two epicyclic gears’ stage, the first stage contains eight planet gears and the second stage with nine planet gears, see Fig. 3. Specifications of the gears are documented in Table 1.

The epicyclic module planet gears are designed as a complete gear and bearing assembly. The outer race of the bearing and the gear wheel is a single component, with the bearing rollers running directly on the inner circumference of the gear. Each planet gear is ‘self-aligning’ by the use of

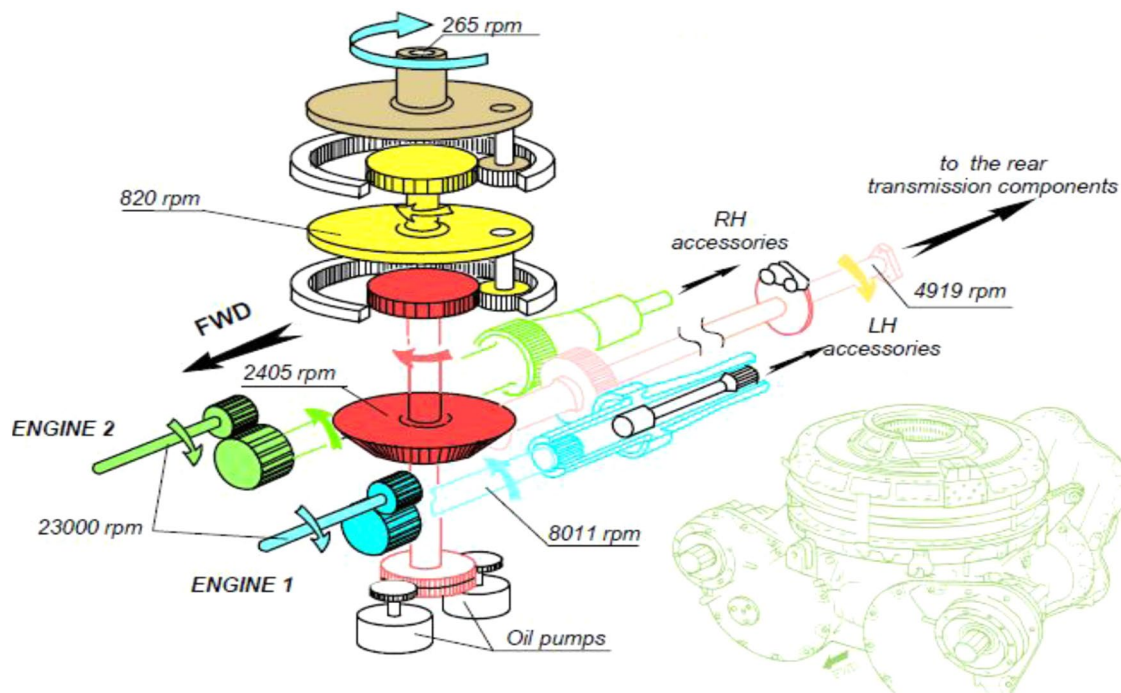


Fig. 2 Gearbox internal parts [24]



**Fig. 3** Second-stage epicyclic gears

spherical inner and outer races and barrel-shaped bearing rollers (see Fig. 3).

**Experimental Conditions and Setup**

The test procedure consists of three experimental conditions, including fault-free condition, minor seeded bearing damage and major seeded bearing defects.

The bearing defects were inserted on one of the planet gears of the 2nd epicyclic stage. The minor defect was simulated by machining a rectangular section with 0.3 mm in depth and 10 mm in width as shown in Fig. 4. The major defect was simulated as a combination of a defected inner race (natural spalling around half of the circumference) and an outer race (around 0.3 mm in depth and 30 mm in width) as shown in Fig. 5. For each fault case, three loading conditions were added to the test rig, 110% of maximum take-off power, 100% and 80% of maximum continuous power. The load condition characteristics were detailed as follows:

- 110% Max take-off power: power 1760 Kw, rotor speed 265 rpm, right input torque 368 Nm and left input torque 368 Nm.
- 100% Max continuous power: power 1300 Kw, rotor speed 265 rpm, right input torque 272 Nm and left input torque 272 Nm.



**Fig. 4** Slot across the bearing outer race

- 80% Max continuous power: power 936 Kw, rotor speed 265 rpm, right input torque 196 Nm and left input torque 196 Nm.

**Data Acquisition and Instrumentation**

In this study, a triaxial accelerometer (type PCB Piezotronics 356A03) was installed to capture MGB vibration signals. The accelerometer captured vibration signals at a sampling frequency of 51.2 kHz and was mounted on the case of the gearbox externally, as shown in Fig. 6. All vibration data were recorded using a National Instruments (NI) NI cDAQ-9188XT CompactDAQ Chassis. A 60-s sample was recorded for each fault condition. The Y-axis of the tri-axial accelerometer arrangement was oriented parallel to the radial direction of the gearbox, the X-axis to the tangential axis, and the Z-axis is the vertical axis parallel to the rotor axis, see Fig. 6.

**Results**

The wavelet packet with five levels and DB function was used to decompose the non-deterministic signal, each *i* decomposition was presented as a node on the decomposition tree.

**Table 1** Tooth numbers for the gearbox gears

First epicyclic module		Second epicyclic module		First parallel stage	Second parallel stage	Bevel stage
Sun gear		Sun gear		Pinion teeth	Pinion teeth	Pinion teeth
62		68		23	35	22
Planet gear—8 gears	Ring gear	Planet gear—9 gears	Ring gear	Wheel teeth	Wheel teeth	Bevel teeth
34	130	31	130	66	57	45



**Fig. 5** Inner race natural spalling

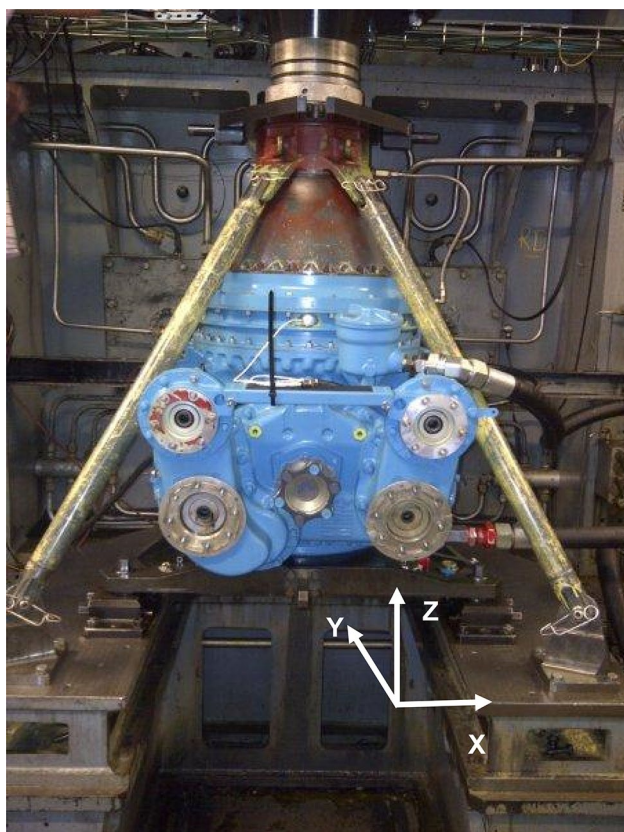


**Fig. 6** MGB installed on the test bench

Then, combination indicator was estimated for the decompositions on the 5th level, and an example of decomposed signals at nodes 5.22, 5.23, and 5.24 is shown in Fig. 7. The decomposition with the highest combination indicator was used to estimate the impulse energy indicator.

Figure 8 shows the combination indicator and kurtosis for the decomposed signals at level 5. Decomposition

with the band between 18,960 and 19,750 has the highest combination indicator (7.4); results of kurtosis showed low response for this frequency range, and the maximum for mid-range frequencies which is not related to the excitation frequency. Therefore, the combination indicator is proposed in this paper to overcome the limitations of maximum kurtosis-based methods. The proposed indicator provides the potential of more accurate fault diagnosis by combining the advantages of kurtosis and RMS in one combined indicator.

### Impulse Energy Condition Indicator (IE)

The results of the IE indicator showed distinctive differences between the healthy and faulty condition with the IE increasing significantly for minor and major faults. The response of the IE indicator was consistent for measurements taken in all directions as shown in Fig. 9, and the IE indicator increased by more than 300% for the minor fault. In addition, distinctions between minor and major fault were observed, especially for the vibration signal acquired at 100% of continuous power where the impulse energy indicator for major fault increased by 100% compared to the minor fault condition.

### Root Mean Square (RMS) Indicator

The results of RMS showed the level of RMS of vibration signal was increased due to the bearing damage; besides, the level of RMS increased as the fault severity increased, the highest level of RMS is corresponding to the major damage whilst the lowest level corresponded to fault-free condition, see Fig. 10. Observation of RMS level showed the sensitivity of the result of the measurement direction, the Y and Z direction of vibration displayed consistent growth of RMS level as fault severity increased. Observations of RMS level calculated for X-direction showed a significant difference between healthy and faulty conditions; however, the X direction results were incapable of measuring the severity of bearing damage. The results showed RMS level depended on the load, and the RMS level increased significantly when the load reached 110% of rated load see Fig. 10a. However, there was no significant difference between rated condition and 80% of rated load condition, see Fig. 10b, c.

### Kurtosis

The results of Kurtosis showed that this indicator was unable to detect the bearing defects. The kurtosis of the vibration signal collected at 110% load condition showed no distinctive difference between fault-free and damage condition, see Fig. 11a. The results of 100% and 80% load condition show high levels of kurtosis for the fault-free condition which can be interpreted incorrectly as bearing damage. Therefore,

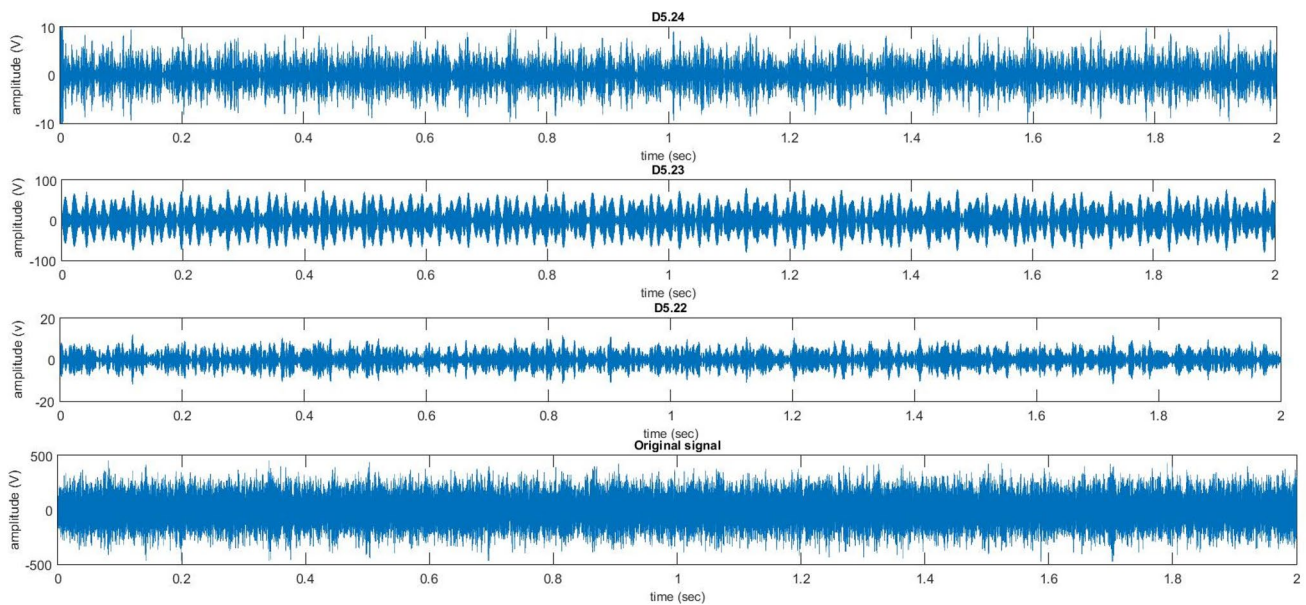
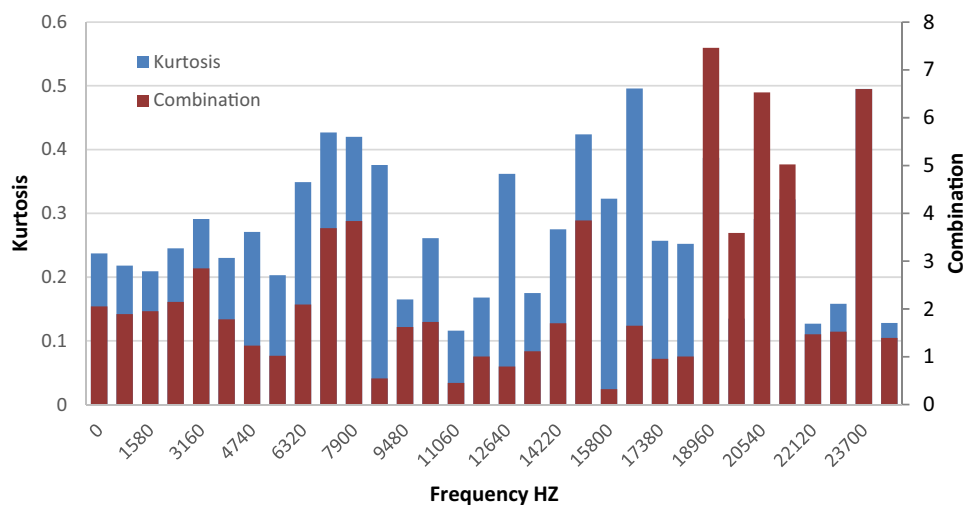


**Fig. 7** Example of the decomposed signal at node 5.22, 5.23 and 5.24 compared to the original signal

**Fig. 8** Combination indicator Vs Kurtosis



using this indicator alone can result in decreasing the confidence of the monitoring system.

### Discussion

The main advantage of signal separation techniques is their ability to improve signal-to-noise ratio where the vibration signal is susceptible to background noise. This makes them more effective in applications where the vibration signals need to go through an arduous transmission path from the outer race through the rollers to the inner race and then the planet carrier. The use of signal separation has contributed significantly to improving the signal-to-noise ratio.

A method for filter band selection has been developed based on signal decomposition using wavelet packet. The wavelet packet decomposition provides valuable information toward extracting the transitory features from non-stationary vibration signals resulted from the defected bearing. Choosing the number of levels is very crucial in band selection, therefore, the authors decided to choose this value based on two criteria; first, the number of decomposition should be larger than the number of levels estimated by wavelet packet decomposition WPD function. Also, the bandwidth of the last decomposition should be larger than the third harmonic of the bearing defect frequency, see [6]. The band selection aims to extract impulses within the non-deterministic signal. The method takes advantage of RMS and kurtosis

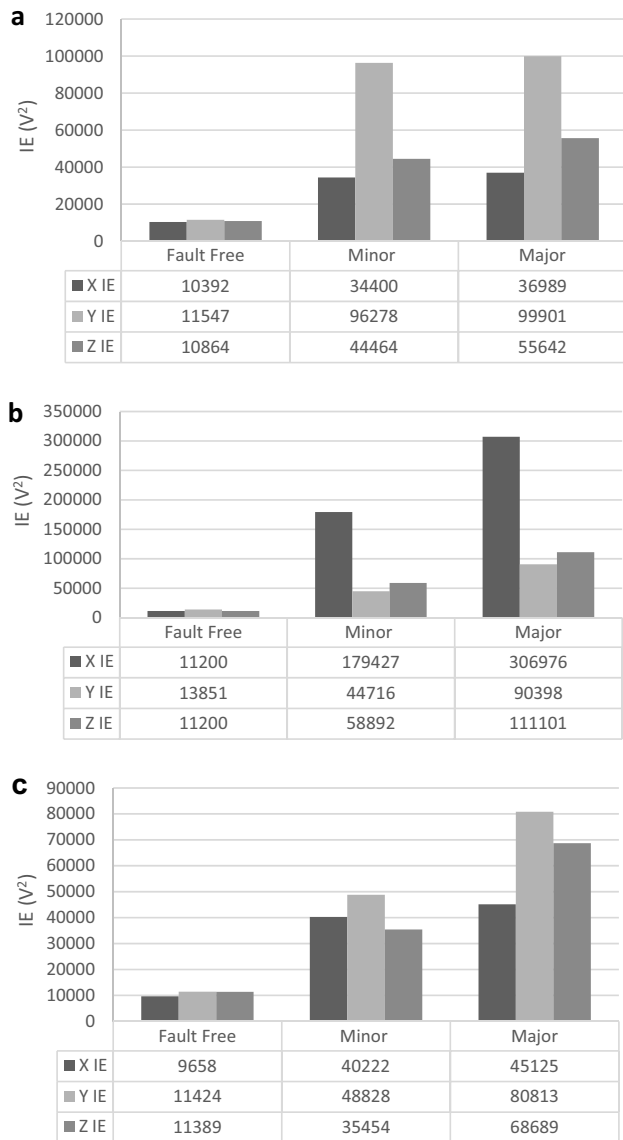


**Fig. 9** IE indicator for vibration signals. **a** 110% max take-off power, **b** continuous power and **c** 80% of continuous power

combination estimated for the lower level of the decomposition tree. Employing the decomposition on one level provided a better computational performance compared to kurtogram methods. The combination indicator good performance due to use of kurtosis and RMS together is indicative of maximum energy of impulsive signal.

The selected band was employed to compute the impulse energy indicator IE and then compared to well-established indicators such as RMS and kurtosis. The IE showed the distinctive difference between healthy, minor and major fault. The high levels associated with the impulse indicator of minor and major defect cases indicate the presence of bearing defects. Moreover, the IE results showed consistent response for different loading conditions, especially for the data acquired

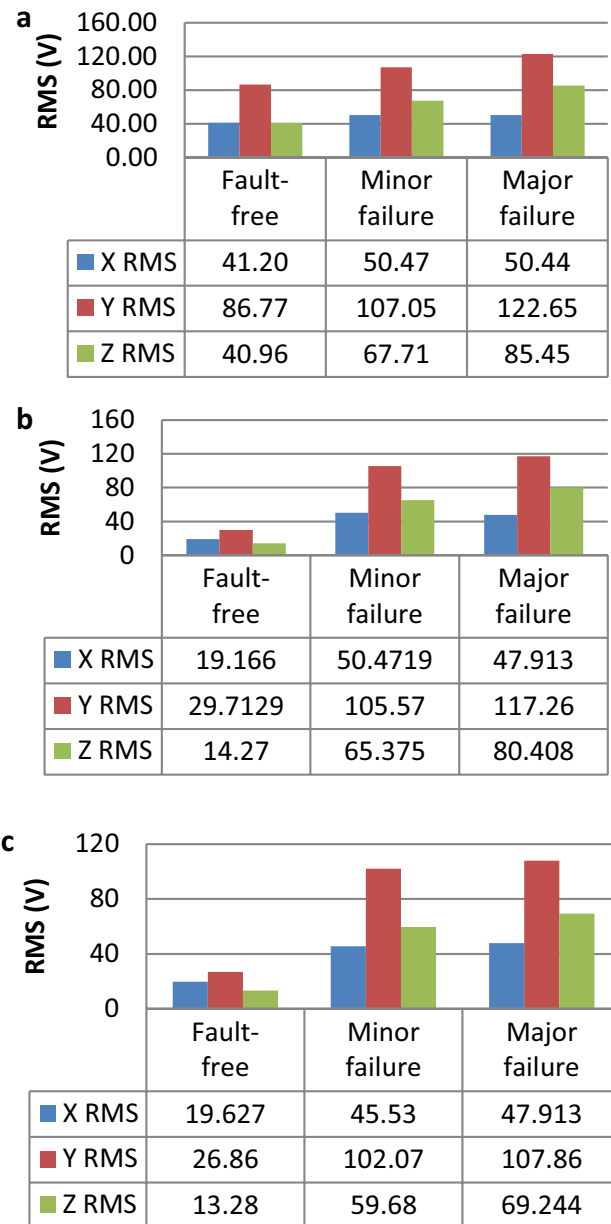


**Fig. 10** RMS of vibration signal. **a** 110% max take-off power, **b** continuous power and **c** 80% of continuous power

in 100% continuous power, in which the IE increased by 100% for the major fault case compared to the minor fault case. In addition, the indicator response was independent of the measurement direction. The result of Kurtosis failed to show distinctive differences amongst all three fault cases. In comparison, the RMS results showed relatively higher values for both the minor and major fault cases. Both RMS and kurtosis were sensitive to the load and measurement direction. Furthermore, RMS showed no distinctive difference between minor and major faults especially for vibration data measured at 100% and 80% of continuous power. Therefore, the results of IE indicator were more robust at indicating damage for both minor and major damage compared to the RMS and kurtosis.



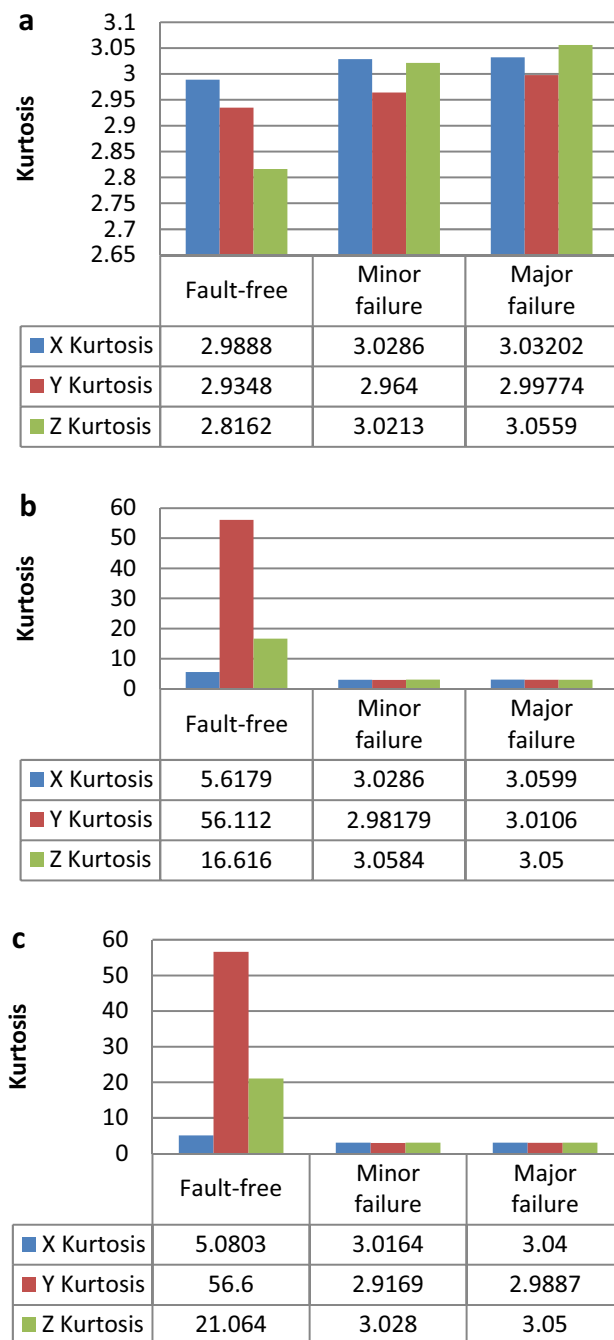


**Fig. 11** Kurtosis of vibration signal. **a** 110% max take-off power, **b** continuous power and **c** 80% of continuous power

## Conclusion

A technique to extract frequency band corresponding the bearing faults impulses has been developed. The technique employs the adaptive filter signal separation, wavelet packet decomposition and the combination of RMS and Kurtosis to select the optimum filter band.

The selected filter band was used to estimate the impulse energy (IE) indicator. The IE indicator has been tested by vibration data collected from the transmission system of a CS-29 ‘Category A’ helicopter gearbox under different bearing damage severity of the second planetary stage. Results showed successful in faults’ detection with this indicator. Also, the IE indicator responds consistently to the fault severity compared to the traditional indicators such as RMS and kurtosis.

Such an indicator has the potential to be used by helicopter health usage and monitoring system to detect bearing faults during flight. Further investigation is required to decide the bearing fault locations such as the outer race or inner race fault.

**Acknowledgements** This study is sponsored by European Aviation Safety Agency (EASA), project entitled “MGH—Helicopter main gearbox health”.

## Compliance with Ethical Standards

**Conflict of interest** The authors declare there is no conflict of interest.

## References

1. Decker HJ (2002) Crack detection for aerospace quality spur gears, NASA/TM-2002-211492, ARL-TR-2682. Glenn Research Center, NASA
2. Samuel PD, Pines DJ (2005) A review of vibration-based techniques for helicopter transmission diagnostics. *J Sound Vib* 282(1–2):475–508
3. Randall RB, Sawalhi N, Coats M (2011) A comparison of methods for separation of deterministic and random signals. *Int J Cond Monit* 1(1):11
4. Antoni J, Randall RB (2001) Optimisation of SANC for separating gear and bearing signals. *Cond Monit Diagn Eng Manag* 1:89–99
5. Randall RB (2004) Detection and diagnosis of incipient bearing failure in helicopter gearboxes. *Eng Fail Anal* 11(2):177–190
6. Ho D, Randall RB (2000) Optimisation of bearing diagnostic techniques using simulated and actual bearing fault signal. *Mech Syst Signal Process* 14(5):763–788
7. Elasha F, Mba D, Ruiz-Carcel C (2016) A comparative study of adaptive filters in detecting a naturally degraded bearing within a gearbox. *Case Stud Mech Syst Signal Process* 3:1–8
8. Elasha F, Ruiz-Carcel C, Mba D, Chandra P (2014) A comparative study of the effectiveness of adaptive filter algorithms, spectral kurtosis and linear prediction in detection of a naturally degraded bearing in a gearbox. *J Fail Anal Prev* 14(5):623–636
9. Randall RB, Antoni J (2011) Rolling element bearing diagnostics—a tutorial. *Mech Syst Signal Process* 25(2):485–520
10. Dwyer R (1983) Detection of non-Gaussian signals by frequency domain kurtosis estimation. In: *Acoustics, speech, and signal processing, IEEE international conference on ICASSP’83, vol 8, IEEE, pp 607*
11. Antoni J, Randall R (2006) The spectral kurtosis: application to the vibratory surveillance and diagnostics of rotating machines. *Mech Syst Signal Process* 20(2):308–331

12. Mauricio A, Smith W, Randall R, Antoni J, Gryllias K (2019) Cyclostationary-based tools for bearing diagnostics of helicopter planetary gearboxes. In: AIAC18: 18th Australian international aerospace congress (2019); HUMS-11th defence science and technology (DST) international conference on health and usage monitoring (HUMS 2019); ISSFD-27th international symposium on space flight dynamics (ISSFD) (p. 837). Engineers Australia, Royal Aeronautical Society
13. Zhou L, Duan F, Corsar M, Elasha F, Mba D (2019) A study on helicopter main gearbox planetary bearing fault diagnosis. *Appl Acoust* 147:4–14
14. Abboud D, Antoni J, Eltabach M, Sieg-Zieba S (2015) Angle/time cyclostationarity for the analysis of rolling element bearing vibrations. *Measurement* 75:29–39
15. Souza P, Souza V, Silveira LF (2019) Analysis of spectral sensing using angle-time cyclostationarity. *Sensors* 19(19):4222
16. Elasha F, Mba D (2016) Improving condition indicators for helicopter health and usage monitoring systems. *Int J Struct Integr* 7(4):584–595. <https://doi.org/10.1108/IJSI-09-2015-0032>
17. Smith JO, Abel JS (1999) Bark and ERB bilinear transforms. *IEEE Trans Speech Audio Process* 7(6):697–708
18. Dentino M, McCool J, Widrow B (1978) Adaptive filtering in the frequency domain. *Proc IEEE* 66(12):1658–1659
19. Ferrara ER (1980) Fast implementations of LMS adaptive filters. *IEEE Trans Acoust Speech Signal Process* 28(4):474–475
20. Alan D (1998) *Handbook of the condition monitoring techniques and methodology*, 1st edn. Chapman and Hall, London
21. Elasha F, Mba D, Kiat CRG, Nze I, Yebra G (2014) Diagnostics of worm gears with vibration analysis. In: 11th international conference on condition monitoring and machinery failure prevention technologies, CM 2014/MFPT 2014
22. Elasha F, Ruiz-Cárcel C, Mba D, Kiat G, Nze I, Yebra G (2014) Pitting detection in worm gearboxes with vibration analysis. *Eng Fail Anal* 42:366–376
23. Sawalhi N, Randall RB, Endo H (2007) The enhancement of fault detection and diagnosis in rolling element bearings using minimum entropy deconvolution combined with spectral kurtosis. *Mech Syst Signal Process* 21(6):2616–2633
24. Department for Transport (2011) Report on the accident to aerospatiale (Eurocopter) AS332 L2 Super Puma, registration G-REDL 11 nm NE of Peterhead, Scotland, on 1 April 2009, 2/2011. Air Accident Investigation Branch, Aldershot

**Publisher's Note** Springer Nature remains neutral with regard to jurisdictional claims in published maps and institutional affiliations.